

## Cavity ringdown heterodyne spectroscopy: High sensitivity with microwatt light power

Jun Ye\* and John L. Hall

*JILA, National Institute of Standards and Technology and University of Colorado, Boulder, Colorado 80309-0440*

(Received 11 January 2000; published 17 May 2000)

We present an ac heterodyne technique in cavity ringdown spectroscopy that permits  $1 \times 10^{-10}$  absorption sensitivity with microwatt-level light power. Two cavity modes, one probing the empty cavity and the other probing intracavity absorption, are excited simultaneously but with their intensities temporally out of phase, with one mode decaying and the other rising. Heterodyne detection between the two modes reveals the dynamic time constants associated with the empty cavity and the additional intracavity gas absorption. The method offers a quick comparison between the on- and off-resonance information, a prerequisite to reaching the fundamental shot-noise limit. This simple and yet important improvement of cavity ringdown spectroscopy should lead to the enhanced performance of a wide range of applications.

PACS number(s): 42.62.Fi; 07.57.Ty; 42.79.Gn; 39.30.+w

The need for high detection sensitivities has stimulated many useful developments in spectroscopic techniques. The use of optical resonators to enhance absorption contrast was suggested early on [1] and realized in cw operations [2,3]. The advent of the popular technique of cavity ringdown spectroscopy (CRDS) [4,5] has pushed this cavity enhancement scheme to many different application areas, such as characterization of high-reflectivity mirrors, measurement of ultraslow reflector velocities, atmospheric sensing and detection of trace species in gas phase environment, absolute determination of absorption band strength and/or species concentration, analysis of combustion and plasma dynamics, and the study of chemical kinetics, such as radical reactions and internal vibration redistribution. Recently, cavity ringdown spectroscopy has been extended to surface and condensed matter [6], permitting a wide range of what we consider novel fundamental investigations.

Inside a high-finesse ( $F$ ) cavity, the light completes many round-trips through the intracavity absorber and effectively increases the interaction length by  $(2F/\pi)$ , a factor that is readily achievable in a straightforward absorption measurement. CRDS explores a different manifestation of the same physical property of the cavity enhancement: It seeks the information about intracavity gas absorption by measuring the change of decay dynamics associated with the cavity field. The unknown absorption coefficient is now compared with the known mirror losses, which could be made on the similar order of magnitude of the quantity to be measured, and thus detection against a large background is avoided and measurement contrast is enhanced. In CRDS, a pulsed operation is utilized where an abrupt termination of the input field to cavity permits a measurement of the exponential decay curve of the cavity-transmitted power. To a large extent this cavity ringdown method avoids the technical noise of light; however, residual fluctuations of the apparent cavity loss itself have prevented this technique from reaching the fundamental noise limit.

Briefly speaking, CRDS has two shortcomings. The first one is that CRDS, in its ordinary form, is basically a dc method. Typically, two decay-time measurements are made,

one on the empty cavity decay and the other on the cavity plus sample. The difference between the two measurements contains the useful information. However, a large separation in time between the two measurements allows slow drift and other technical noises to contaminate the data. The second problem is that in order to map out the whole decay curve, a huge dynamic range is needed for the detection instrument to record the data. It is common in CRDS for the last portion of the exponential decay curve to be masked by instrumental noise simply because insufficient light power is left (after some decay) to dominate over electronic noise. For this purpose, Levenson *et al.* [7], introduced a large local oscillator field to be superposed with the decay field so that the resultant beat signal can always be light-noise limited. In this Rapid Communication, we intend to use our ac heterodyne techniques to address both issues at the same time.

To measure a small change of signal in a varying background requires a careful process of signal extraction and averaging. One often employs a modulation technique to compare the signal against the background in short time intervals so that any drifts and noise in the background can be accurately subtracted off. In our earlier work, we combined the frequency-modulation (FM) technique with the cavity and achieved basically the shot-noise limited absorption sensitivity in sub-Doppler resolution [8]. In that case, the on- and off-resonance information was compared effectively at a radio frequency (rf), which is located far enough away from the laser intensity noise spectrum. In the present work, the comparison of the two slightly different time constants, one associated with an empty cavity and the other with additional loss, is not performed in the rf domain. However, with the aid of cavity filtering and an intensity-stabilized laser we are nearly (within a factor of 4) at the fundamental quantum noise limit in cavity enhanced linear spectroscopy.

Figure 1 illustrates the basic scheme of our method. An intensity-stabilized cw laser beam is split by two acousto-optic modulators (AOMs) into two beams with an impressed 1.3-GHz frequency offset; i.e.,  $\Omega_1 - (-\Omega_2) = 1.3$  GHz. This offset is chosen so that both beams can resonate with the cavity simultaneously [four mode orders apart, cavity free-spectral-range (FSR) frequency 318.34 MHz,  $F \sim 90\,000$ ]. After being combined and mode coupled into the cavity, the two beams give 3  $\mu$ W each in cavity transmission. However,

\*FAX: (303) 492-5235. Electronic address: ye@jila.colorado.edu

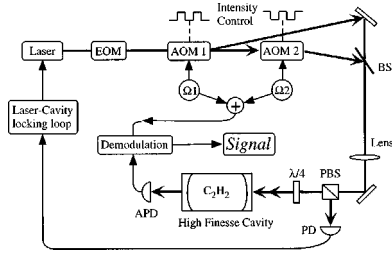


FIG. 1. Experimental setup for the chopped heterodyne ringdown spectroscopy. The two AOMs provide the necessary frequency offset between the two modes and are chopped out of phase. The laser is locked on the cavity since there is always one beam on. The heterodyne beat between the two modes at the cavity transmission is demodulated against the known carrier frequency to produce the decay signal. PD, photodiode; APD, avalanche photodiode.

their intensities are chopped out of phase by their respective AOMs such that only one beam is presented to the cavity input at one time. Despite the switching, a detector viewing the cavity reflection is able to maintain the laser/cavity lock using the Pound-Drever-Hall technique [9], with the rf sideband generated by the electro-optics modulator (EOM). Inside the cavity, there are of course one decaying mode and one rising mode; i.e., within the time scale of the order of cavity ringdown, the cavity mode that is currently being coupled in will rise exponentially while the other mode, with its input switched off, will decay exponentially. At the cavity transmission, we can detect the heterodyne beat wave form between the two modes. Demodulation against the known carrier frequency (1.3 GHz) will then reveal the heterodyne beat amplitude, which contains the information of dynamic variation of both modes. For an empty cavity, the beat amplitude wave form remains unchanged at neighboring chopping cycles. However, when one of the modes is tuned to a molecular resonance, the system exhibits two slightly different time constants associated with the two modes. The beat wave form becomes asymmetric between the neighboring chopping cycles, and their difference is related to the intracavity absorption. The period of the chopping cycle can be chosen to roughly match the field decay time ( $1/e$ ) of the empty cavity. This technique thus offers a quick comparison of on- and off-resonance information and substantially suppresses technical noises associated with both light and cavity. Since each ringdown wave form is registered only up to one chopping period, is on the order of  $1/e$  field decay time, we completely avoid the necessity of reserving a few decades of dynamical range to record signals.

To illustrate the previous discussion further in detail, we present a simple theoretical model for this technique. Suppose the round-trip loss of the empty cavity is  $L_{\text{cav}}$ , the round-trip absorption of the intracavity medium is  $A$ , and the round-trip time of light is  $t_{\text{round-trip}}$ . For a cavity mode that is far detuned from the medium resonance, the characteristic time constant associated with the mode dynamics is given by

$$\tau_{\text{cav}} = 2t_{\text{round-trip}}/L_{\text{cav}}. \quad (1)$$

We stress that this is the  $1/e$  decay time of the field, a relevant quantity since we deal with heterodyne detection be-

tween two fields. For the mode that is tuned to the absorption peak of the medium, the decay time constant becomes

$$\tau_{\text{abs}} = 2t_{\text{round-trip}}/(L_{\text{cav}} + A). \quad (2)$$

Following the intensity-chopping scheme of Fig. 1, let us assume that during the period of  $[0, \Delta t/2]$ , mode 1 ( $E_1$ ) of the empty cavity is switched on while mode 2 ( $E_2$ ), which sees the additional intracavity absorption, is switched off. After some cycles, the two field amplitudes evolve as

$$E_1 = c_1 [1 + \exp(-\Delta t/2\tau_{\text{cav}}) - \exp(-t/\tau_{\text{cav}})], \quad (3)$$

$$E_2 = c_2 \exp(-t/\tau_{\text{abs}}).$$

Here  $c_1$  and  $c_2$  are amplitude coefficients for  $E_1$  and  $E_2$ , respectively. In the next half cycle,  $[\Delta t/2, \Delta t]$ , we reverse the two fields such that mode 1 is switched off and mode 2 on. The product of the two-field amplitudes is what we detect in the demodulated signal of the cavity transmitted heterodyne beat. If we compare the signal of the two neighboring half cycles, we obtain the information of absorption:

$$(E_1 E_2)_{[0, \Delta t/2]} - (E_1 E_2)_{[\Delta t/2, \Delta t]} = c_1 c_2 [(1 + e^{-\Delta t/2\tau_{\text{cav}}})e^{-t/\tau_{\text{abs}}} - (1 + e^{-\Delta t/2\tau_{\text{abs}}})e^{t/\tau_{\text{cav}}}]. \quad (4)$$

Figure 2 shows the results obtained from Eqs. (3) and (4). The chopping period  $\Delta t$  is chosen to be  $4\tau_{\text{cav}}$ , and the time axes have been normalized to  $\tau_{\text{cav}}$ . For an empty cavity, shown in the right column, the switched wave forms of mode 1 and mode 2 are symmetric, resulting in a uniform beat amplitude between neighboring half cycles and thus the zero baseline. When mode 1 and mode 2 “see” different intracavity loss, as shown in the left column of the figure, there is a clear asymmetry in the beat amplitudes between the neighboring half cycles; their differences, as plotted in the bottom curve, show the level of additional absorption. In this case, the medium absorption is 10% of the empty cavity losses.

The fundamental limit of the obtainable sensitivity of this method follows nicely from Eqs. (3) and (4). Suppose the two modes have the same amplitude coefficients,  $c_1 = c_2 = \sqrt{P_0}$ , in transmission, and the light is converted to a photocurrent according to  $i = \eta P$ , where  $\eta$  is the detector responsivity (A/W). The demodulated beat current is  $\eta \times 2E_1 E_2 / \sqrt{2}$ . For the simplicity of presentation, we use the small absorption limit,  $\tau_{\text{cav}} \approx \tau_{\text{abs}}$ , and assume  $\Delta t/\tau_{\text{cav}} \geq 10$ . The difference signal of Eq. (4) becomes

$$\begin{aligned} i_{\text{signal}} &\sim \eta (2/\sqrt{2}) P_0 [e^{-t/\tau_{\text{abs}}} - e^{-t/\tau_{\text{cav}}}] = -\eta\sqrt{2} P_0 e^{-t/\tau_{\text{cav}}} \\ &\quad \times [1 - e^{-t(1/\tau_{\text{abs}} - 1/\tau_{\text{cav}})}] \\ &= -\eta\sqrt{2} P_0 (1/\tau_{\text{abs}} - 1/\tau_{\text{cav}}) t e^{-t/\tau_{\text{cav}}}. \end{aligned} \quad (5)$$

Since the beat amplitude reaches the maximum when  $E_1 = E_2$ , therefore we have  $\exp(-t/\tau_{\text{cav}}) \approx 1/2$  and  $t = \tau_{\text{cav}} \ln 2$ . With the help of Eqs. (1) and (2),

$$i_{\text{signal}} = -\eta\sqrt{2} P_0 \tau_{\text{cav}} \frac{\ln 2}{2} \frac{A}{2t_{\text{round-trip}}} = -\eta P_0 \frac{\ln 2}{\sqrt{2}} \frac{A}{L_{\text{cav}}}. \quad (6)$$

The shot noise produced by the dc photocurrent,  $i_{\text{dc}} = \eta$

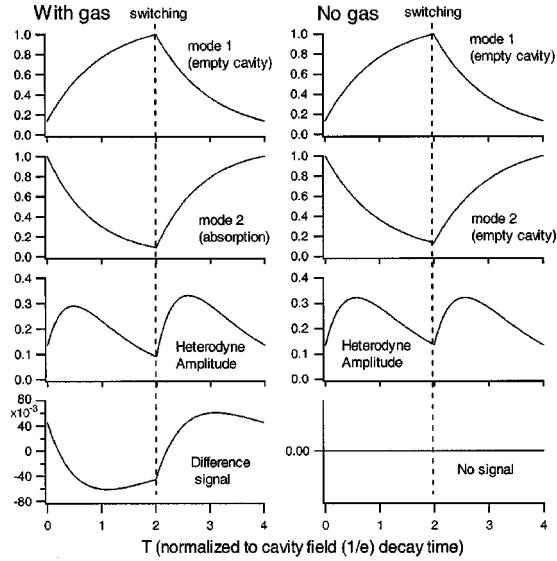


FIG. 2. Comparison of the demodulated ringdown curve between the empty cavity (right column) and the cavity with extra absorption (left column). The chopping period  $\Delta t = 4\tau_{\text{cav}}$  and the time axes are normalized to  $\tau_{\text{cav}}$ . From top to bottom, we show, respectively, the switching dynamics of mode 1, mode 2, their product (beat), and the difference signal between the neighboring half cycles.

$\times 2(\sqrt{P_0}/2)^2 = \eta P_0/2$ ,  $i_{\text{noise}} = \sqrt{2eB\eta P_0/2}$ , where  $e$  is the electron charge and  $B$  the detection bandwidth. The resultant  $S/N$  is

$$|i_{\text{signal}}/i_{\text{noise}}|_{\text{shot noise}} = \sqrt{\eta P_0/eB} (\ln 2/\sqrt{2}) (A/L_{\text{cav}}). \quad (7)$$

In terms of the noise equivalent sensitivity of single pass integrated absorption, we set  $S/N=1$ , and

$$\left(\frac{A}{2}\right)_{\text{min}} = \frac{\sqrt{2}}{\ln 2} \sqrt{\frac{eB}{\eta P_0}} \frac{L_{\text{cav}}}{2} = \frac{\sqrt{2}}{\ln 2} \sqrt{\frac{eB}{\eta P_0}} \frac{\pi}{F}. \quad (8)$$

This sensitivity result is basically the same as that expressed in Eq. (3) of Ref. [8] except for a small numerical factor ( $\sim 2$ ), an expected result since both methods are shot-noise limited. The difference arises from the fact that in the cavity-enhanced frequency modulation spectroscopy, some portion of the carrier power is converted to the sidebands, leading to a slight loss of sensitivity for a fixed total optical power.

The experiment uses a Yb:YAG laser to probe acetylene gas filled inside our high finesse cavity. The transition involved is a vibration overtone line [10]:  $\text{C}_2\text{H}_2(3\nu_3)R(29)$ , located at 1031.6528 nm, with an absorption coefficient of  $4 \times 10^{-6}/\text{Torr cm}$ . For our 46.9-cm-long cavity, we typically use an intracavity pressure of a few mTorr (1 Torr=133 Pa) for a  $1 \times 10^{-6}$  level of absorption. The beam chopping frequency is chosen at 1.4 kHz, corresponding to  $\Delta t = 714 \mu\text{s}$ . The cavity transmission is received by an avalanche photodiode (APD) and the beat signal is sent to an rf spectrum analyzer for demodulation [11]. To measure the empty cavity finesse, we first tune both mode 1 and mode 2 out of the molecular resonance. Figure 3 shows a representative trace of the demodulated heterodyne beat ringdown wave form with an overlaid theoretical fit. The simple model presented

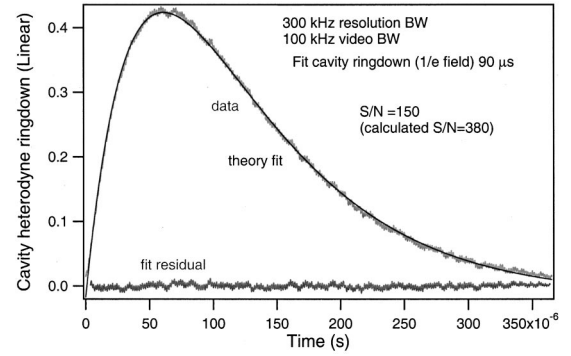


FIG. 3. A representative trace of the chopped ringdown curve of the empty cavity, obtained from the video output of the rf spectrum analyzer. A theoretical fit and the fit residual are also shown.

above produces an excellent fit, giving the empty cavity field ringdown ( $1/e$ ) time of  $90 \mu\text{s}$ . This leads to a cavity linewidth (full width at half maximum) of 3.5 kHz and a finesse of 90 000. Within the detection bandwidth (BW) of 173 kHz (resolution BW 300 kHz and video BW 100 kHz), the recovered  $S/N$  is 150, about two times smaller than the expected value. This is partly due to the “ringing” noise of the spectrum analyzer’s rf filter function, which is optimized for the frequency domain analysis. To avoid distortion of the ringdown signal, it is not feasible to use a smaller BW on the instrument.

We then tune mode 2 to the center of the acetylene resonance and the ringdown wave form becomes clearly asymmetric in the neighboring half cycles. Figure 4 shows a set of experimental data where we vary the intracavity gas pressure to generate four different absorption levels (expressed in terms of single pass in the graph). Their respective ringdown beat wave forms are shown in the left column of the figure. The absorption data (shown in the right column) are produced in the following way. We first generate a copy of the original data and then shift their time axes by a half chopping cycle. The differences between the original data and the shifted data give the absorption signals. With a single pass absorption of  $1.7 \times 10^{-6}$ , the acquired  $S/N$  is 10 with a BW of 173 kHz. The absorption sensitivity normalized to a 1-s averaging time is then  $1.6 \times 10^{-10}$ . At a steady state (no chopping), each mode has  $3 \mu\text{W}$  ( $P_0$ ) in the cavity transmission.  $\eta$  of the APD is 0.3 A/W. The shot-noise limited sensitivity of Eq. (8) is then  $\sim 1.2 \times 10^{-11}$  at 1-s averaging. However, since the APD has an excess noise factor of  $\sim 3$ , the expected minimum absorption sensitivity should in fact be  $\sim 4 \times 10^{-11}$ , a factor of 4 lower than our experimental result.

One notices in Fig. 4 that the recovered signal amplitude does not increase linearly with respect to the additional intracavity absorption. Of course one can expect that if the gas absorption greatly exceeds the level of the empty cavity loss, sensitivity saturation could occur. In Fig. 5(a), the signal contrast is shown against the intracavity absorption normalized to the empty cavity loss. The dotted curve is calculated assuming that the coupling power to mode 2 (the absorbing mode) remains a constant. However, we know that with added loss inside, the power coupling efficiency to the cavity changes and the available power for mode 2 decreases.

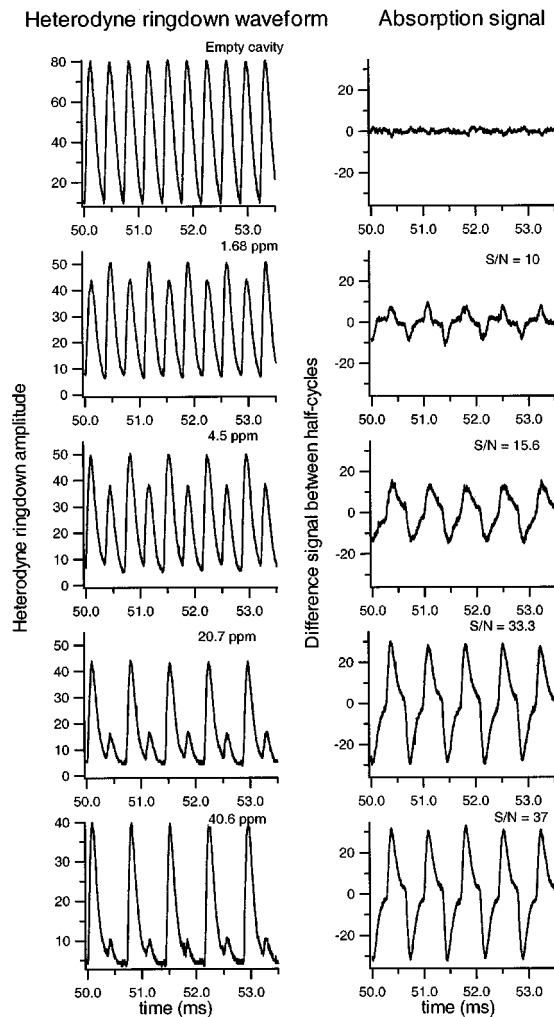


FIG. 4. Demodulated heterodyne beat amplitudes between the two chopped cavity modes (left column) in the presence of intracavity absorption (labeled in the graph). Shown in the right column is the absorption signal obtained by differencing the beat amplitudes in the neighboring half cycles.

Therefore for a fixed incident power, the sensitivity saturation occurs sooner. This is the scenario plotted in the solid curve of Fig. 5(a). Figure 5(b) illustrates saturation of the experimental data of Fig. 4. The model from Fig. 5(a) is used to fit the data. To solve the problem of saturation, an obvious solution is to maintain appropriate mode coupling as the intracavity absorption level rises. We can also use faster chopping cycles.

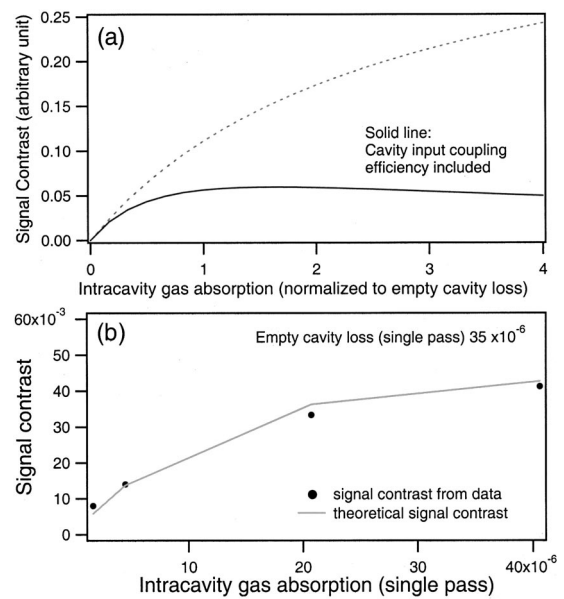


FIG. 5. (a) Signal contrast vs intracavity molecular absorption. The change of cavity input coupling efficiency is (not) taken into account in the solid (dotted) curve. (b) Experimental data from Fig. 4, showing signal saturation when the molecular absorption approaches the empty cavity loss ( $35 \times 10^{-6}$  single pass).

In summary, we have presented an ac technique in cavity ringdown spectroscopy that should enable shot-noise-limited detection in the linear absorption measurement. A detection sensitivity of  $1.6 \times 10^{-10}$  at 1-s averaging time is obtained. We believe that the method presented here should prove to be simple and applicable to a wide range of applications, particularly for spectra taken under Doppler—or atmospheric pressure—broadened conditions.

Further improvement of the system includes the use of faster chopping cycles and the replacement of the APD with a sensitive *p-i-n* diode in a resonant matching circuit. At present, the chopping frequency is limited by the locking loop between the laser and the cavity. An alternative is to stabilize the laser on the cavity with a third mode, completely off from the molecular resonance and independent of the other two modes. The third mode can be left on at all times to maintain the lock while the switching can go on as before between the first two modes. A hybrid of our on-resonance/off-resonance switch with transmission heterodyne detection against the third mode is another clear avenue for high sensitivity detection.

We thank L.-S. Ma for useful discussions. The work at JILA is supported by NIST and NSF.

- [1] A. Kastler, *Appl. Opt.* **1**, 17 (1962).
- [2] P. Cerez *et al.*, *IEEE Trans. Instrum. Meas.* **29**, 352 (1980).
- [3] L.-S. Ma and J. L. Hall, *IEEE J. Quantum Electron.* **26**, 2006 (1990).
- [4] D. Z. Anderson *et al.*, *Appl. Opt.* **23**, 1238 (1984).
- [5] A. O'Keefe and D. A. G. Deacon, *Rev. Sci. Instrum.* **59**, 2544 (1988).
- [6] A. C. R. Pipino, *Phys. Rev. Lett.* **83**, 3093 (1999).

- [7] M. D. Levenson *et al.*, *Chem. Phys. Lett.* **290**, 335 (1998).
- [8] J. Ye *et al.*, *J. Opt. Soc. Am. B* **15**, 6 (1998).
- [9] R. W. P. Drever *et al.*, *Appl. Phys. B* **31**, 97 (1983).
- [10] J. Ye, L.-S. Ma, and J. L. Hall, *J. Opt. Soc. Am. B* (to be published).
- [11] The time base of the rf spectrum analyzer is tied to the rf signals used to drive the two AOMs. The video output of the spectrum analyzer in zero-span mode provides demodulation for the heterodyne beat.